

Superconductivity in $LnFePO$ ($Ln = La, Pr,$ and Nd) single crystals

R. E. Baumbach, J. J. Hamlin, L. Shu, D. A. Zocco,
N. M. Crisosto, M. B. Maple

Department of Physics and Institute for Pure and Applied Physical Sciences,
University of California, San Diego, La Jolla, CA 92093

E-mail: mbarcode@ucsd.edu

Abstract. Single crystals of the compounds $LaFePO$, $PrFePO$, and $NdFePO$ have been prepared by means of a flux growth technique and studied by electrical resistivity, magnetic susceptibility and specific heat measurements. We have found that $PrFePO$ and $NdFePO$ display superconductivity with values of the superconducting critical temperature T_c of 3.2 K and 3.1 K, respectively. The effect of annealing on the properties of $LaFePO$, $PrFePO$, and $NdFePO$ is also reported. The $LnFePO$ ($Ln =$ lanthanide) compounds are isostructural with the $LnFeAsO_{1-x}F_x$ compounds that become superconducting with T_c values as high as 55 K for $Ln = Sm$. A systematic comparison of the occurrence of superconductivity in the series $LnFePO$ and $LnFeAsO_{1-x}F_x$ points to a possible difference in the origin of the superconductivity in these two series of compounds.

1. Introduction

Although the rare-earth transition metal phosphide oxides $LnFePO$, where Ln is a lanthanide, were first synthesized in 1995 [1], it was not until 2006 [2] that superconductivity near 5 K was discovered in $LaFePO$. The subsequent report of superconducting critical temperature T_c values near 26 K in the related, fluorine-doped compound $LaFeAsO_{1-x}F_x$ [3] resulted in a great deal of excitement and many publications on what is now recognized as a new class of Fe-based high temperature superconductors. Several different types of doping have been found to induce superconductivity in these compounds including substituting F for O [3, 4, 5, 6, 7, 8, 9], Co for Fe [10], Sr for La [11], Th for Gd [12], and also the introduction of oxygen vacancies [9, 13]. Materials with related structures which include the same type of Fe- Pn planes such as $Ba_{1-x}K_xFe_2As_2$ [14] and $LiFeAs$ [15] have also been found to exhibit similar physics including relatively high temperature superconductivity. Clearly, there exists an enormous phase space of potential Fe- Pn superconductors. The vast majority of work has focused on the arsenic-based versions of these compounds since, thus far, they exhibit the highest T_c values, with the record high T_c near 55 K for $SmFeAsO_{1-x}F_x$ [8] and $SmFeAsO_{1-\delta}$ [13], and 56 K for $Gd_{1-x}Th_xFeAsO$ [12]. Given the toxic nature of arsenic, it would be highly desirable to discover similarly high T_c values in less toxic P-, Sb-, or Bi-based versions of these compounds. However, despite the fact that replacing La with the lanthanides Ce, Pr, Nd, Sm, or Gd in the As-based oxypnictides leads to a near doubling of T_c , there appears to be a striking lack of data on the corresponding phosphorus based versions of these compounds. Although $LaFePO$ has received substantial attention, $SmFePO$ was recently been reported to be superconducting [16], and $CeFePO$ remains non-superconducting down to 400 mK [17], the compounds $LnFePO$ with $Ln = Pr, Nd, \text{ and } Gd$ do not yet appear to have been scrutinized for the occurrence of superconductivity.

The undoped parent compounds, $LnFeAsO$, exhibit a spin density wave (SDW) and structural instability near 150 K, remain metallic to low temperatures, and only display superconductivity when the SDW is suppressed towards zero temperature either through doping or pressure [18]. In contrast, the phosphorus-based analogues $LaFePO$ and $SmFePO$ [16] do not manifest a SDW transition and appear to develop a superconducting state in the undoped form at ambient pressure. Three key questions are whether the mechanism of superconductivity is the same in the P- and As- based compounds, whether the P-based versions of these compounds indeed exhibit superconductivity in the undoped form or only in samples that are in fact of the form $LnFePO_{1-\delta}$, and to what degree sample quality effects the superconducting properties.

For $LaFePO$, values of T_c that range from 3 K [2] to 7 K [19] have been reported. Under pressure, we found that the T_c of $LaFePO$ reaches nearly 14 K at ~ 110 kbar [20]. However, in a recent study of polycrystalline materials, it was concluded that stoichiometric $LaFePO$ is metallic but non-superconducting [21] at temperatures as low as 0.35 K. Our recent work on single crystalline $LaFePO$ [20] indicated T_c values

near 6 K as measured by electrical resistivity and magnetization, but the specific heat exhibited no discontinuity at T_c leading us to propose that the superconductivity may be associated with oxygen vacancies that alter the carrier concentration in a small fraction of the sample, although superconductivity characterized by an unusually small gap value could not be ruled-out. Yet, the superconductivity appeared to be associated with the ZrCuSiAs structure, since the upper critical field was anisotropic. However, in a recent study of single crystals of LaFePO [22], a specific heat anomaly roughly 60% of the expected BCS value in magnitude at the $T_c \approx 6$ K was reported, indicating that the superconductivity can be a bulk phenomenon in this material. These samples were grown using a slightly different method than the one we have employed, where La_2O_3 was used as the oxygen containing precursor rather than Fe_2O_3 , as used in our growths. The variation in the reported data indicate that the T_c value and superconducting fraction are sensitive to the details of the synthesis conditions.

In this paper, we report the results of electrical resistivity, magnetic susceptibility, and specific heat measurements on single crystal samples of LaFePO, PrFePO, and NdFePO. All three compounds exhibit complete resistive superconducting transitions; i.e., the resistivity drops to a negligibly small value at low temperatures. However, as-grown crystals of PrFePO and NdFePO do not show superconducting transitions in the magnetic susceptibility and magnetic screening only develops after post-annealing the samples in flowing O_2 at 700 °C. Annealing in flowing O_2 at 700 °C for 24 hours is also found to improve the superconductive properties of LaFePO.

2. Experimental Details

Single crystals of LaFePO, PrFePO, and NdFePO were grown from elements and elemental oxides with purities $> 99.9\%$ in a molten Sn:P flux. The growths took place over a 1 week period in quartz ampoules which were sealed with 75 torr Ar at room temperature. The inner surface of each quartz ampoule was coated with carbon by a typical pyrolysis method. The starting materials were Ln , Fe_2O_3 , P, and Sn, which were combined in the molar ratios 9:3:6:80.5, similar to previous reports [20, 23] for P-based oxypnictide single crystals. The Fe_2O_3 powder was dried for ~ 10 hours at 300 °C before weighing. The ampoule was heated to 1135 °C at a rate of 35 °C/hr, kept at this temperature for 96 hours, and then rapidly cooled to 700 °C. After removing the majority of the flux by spinning the ampoules in a centrifuge, LaFePO, PrFePO, and NdFePO single crystal platelets of an isometric form with typical dimensions of $\sim 0.5 \times 0.5 \times 0.05 \text{ mm}^3$ or smaller (particularly for the NdFePO crystals), were collected and cleaned in hydrochloric acid to remove the flux from the surface of the crystals prior to measurements. As previously reported [20], the platelets cleaved easily in the ab -plane and were notably malleable, in contrast to the cuprate superconductors. In order to explore the effects of annealing in oxygen, several batches of crystals were heated to 700 °C for 24 hours under flowing O_2 . Hereafter, these samples will be referred to as “ O_2 -annealed”.

X-ray powder diffraction measurements were made using a diffractometer with a non-monochromated $Cu K\alpha$ source to check the purity and crystal structure of the $LaFePO$ and $PrFePO$ single crystals. Due to a small batch yield, x-ray diffraction measurements were not made for the $NdFePO$ crystals. As reported previously, the crystals were difficult to grind into a fine powder as a result of their malleability. Thus, the powder diffraction patterns for $Ln = La$ and Pr crystals were generated from a collection of several crystals which were cut into small pieces using a razor blade and then ground into a coarse powder using a mortar and pestle. The XRD results revealed diffraction patterns that are consistent with those reported previously [1]. Chemical analysis measurements were also made using an FEI Company Model 600 scanning electron microscope which revealed that the stoichiometry for the crystals was consistent with the ratio 1:1:1:1 for $Ln:Fe:P:O$ where $Ln = La, Pr, Nd$.

Electrical resistivity $\rho(T)$ measurements were performed in a four-wire configuration with the current in the ab -plane, at temperatures $T = 1.1\text{-}300$ K using a conventional 4He cryostat and a Quantum Design Physical Properties Measurement System (PPMS). Due to the small size of the crystal samples and uncertainties in the placement of the leads, the absolute resistivity values are accurate only to $\sim \pm 50\%$. Specific heat $C(T)$ measurements were made for 2-300 K for $LaFePO$ and $PrFePO$ crystals in a Quantum Design PPMS semiadiabatic calorimeter using a heat-pulse technique. The specimens for specific heat measurements were attached to a sapphire platform with a small amount of Apiezon N grease and were composed of several hundred single crystals for which the mass $m = 13.06$ mg (La unannealed), 8.93 mg (Pr unannealed), and 6.32 mg (Pr O_2 -annealed). DC magnetization $M(T, H)$ measurements were made using a Quantum Design Magnetic Properties Measurement System (MPMS) in order to probe both the superconducting and normal state properties of the single crystal platelets. For the normal state measurements to room temperature, the $LaFePO$ and $PrFePO$ specimens studied were the same as those used for specific heat measurements and were mounted in cotton packed gelatin capsules. For $NdFePO$, the normal state measurements were made using a single crystal ($m = 0.0125$ mg) which was mounted on a piece of tape with the ab -plane perpendicular to the applied magnetic field. To study the superconducting state, individual single crystal specimens were mounted with the ab -plane perpendicular to the magnetic field. Multiple single crystal platelets were each individually measured for 2-10 K and $H = 5$ Oe under both zero field cooled (ZFC) and field cooled (FC) conditions in order to characterize batch homogeneity via variation in T_c , which was found to be minimal.

3. Results

The electrical resistivity data for unannealed $LnFePO$ ($Ln = La, Pr, \text{ and } Nd$), shown in figure 1, reveal metallic behavior where $\rho(T)$ decreases with decreasing T until the onset of the zero resistance state at the superconducting transition temperatures $T_c \sim 6.6$ K, 3.2 K, and 3.1 K for $Ln = La, Pr, \text{ and } Nd$ respectively. The transition temperatures

Table 1. A summary of results from electrical resistivity measurements for the compounds $LnFePO$ where $Ln = La, Pr, \text{ and } Nd$. The listed quantities are defined in the text and are abbreviated as the following: superconducting transition temperature T_c , width of the superconducting transition ΔT_c (K), residual resistivity ρ_0 (equation 1), quadratic coefficient A (equation 1), and residual resistivity ratio $RRR = \rho_{300K}/\rho_0$.

Ln	T_c (K)	ΔT_c (K)	ρ_0 ($\mu\Omega\text{cm}$)	A ($\mu\Omega\text{cmK}^{-2}$) $\times 10^{-3}$	RRR
La	6.6	1.3	14.0	9.46	32
Pr	3.2	2.0	21.0	5.66	14
Nd	3.1	3.1	13.9	8.28	28

are defined as the T where $\rho(T)$ drops to 50% of the extrapolated normal state value. The transition widths are taken as the difference in the temperatures where $\rho(T)$ drops to 10% and 90% of the extrapolated normal state value. For 100-300 K, the $\rho(T)$ data have approximately linear T dependences which evolve into quadratic forms for $T \sim 10$ -100 K, as shown in the right inset to figure 1. Fits over this temperature range show that the data are well described by the expression,

$$\rho(T) = \rho_0 + AT^2 \quad (1)$$

Additionally, the residual resistivity ratios $RRR = \rho(300K)/\rho(0)$ for unannealed samples are large, reflecting the high quality of the crystals. The results from fits to the $\rho(T)$ data are given in table 1.

Specific heat divided by temperature C/T versus T data for unannealed LaFePO and PrFePO and O_2 -annealed PrFePO are shown in figure 2. From room T , the unannealed $LnFePO$ ($Ln = La, Pr$) specimens exhibit weak increases in C/T with decreasing T that are followed by broad maxima near 110 K (La) and 90 K (Pr). Below its maximum, C/T for LaFePO continues to decrease with decreasing T and is described for $2 \text{ K} < T < 8 \text{ K}$ by a sum of electronic and lattice terms,

$$C/T = \gamma + \beta T^2 \quad (2)$$

yielding an electronic specific heat coefficient $\gamma = 12.7 \text{ mJ/mol-K}^2$ and $\beta = r1944(T^3/\Theta_D)^3 \text{ J/mol-K}$, which gives a Debye temperature $\Theta_D = 268 \text{ K}$.

In contrast to results for LaFePO, C/T versus T data for PrFePO specimens exhibit a trough-peak structure with minima near 27 K and 32 K and maxima near 14.5 K and 15.5 K for unannealed and O_2 -annealed samples, respectively. This type of behavior is indicative of crystalline electric field (CEF) splitting of energy levels of the Pr^{3+} ions, which appears in specific heat data as a so-called ‘‘Schottky anomaly’’. Thus, for $2 \text{ K} < T < 45 \text{ K}$, the $C(T)/T$ data for both unannealed and O_2 -annealed PrFePO specimens were fit by an expression that includes electronic, lattice, and Schottky terms given by,

$$C/T = \gamma + \beta T^2 + rC_{\text{Sch}}/T \quad (3)$$

where γ is the electronic specific heat coefficient and βT^2 represents the lattice contribution to the specific heat. The term $C_{\text{Sch}}(T)$ is the Schottky specific heat anomaly

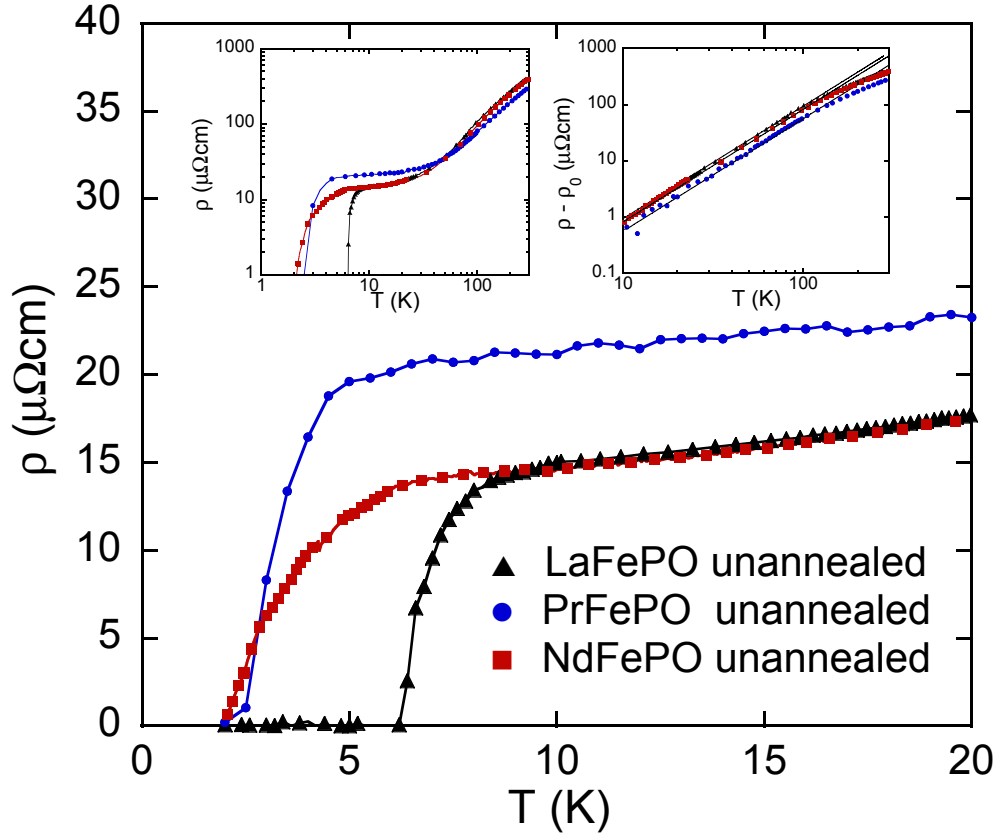


Figure 1. Electrical resistivity ρ versus temperature T measured in the ab -plane for unannealed single crystals of LaFePO, PrFePO, and NdFePO. Left inset: Log-log plot of ρ versus T over the entire measured temperature range. Right inset: Log-log plot of $\rho - \rho_0$ versus T . The solid lines are fits to the data which demonstrate the T^2 behavior for 10-100 K.

for a two-level system arising from the energy difference between the CEF ground state and the first excited state, scaled by a factor r , and is given by,

$$C_{\text{Sch}}(T) = R \left(\frac{\delta}{T} \right)^2 \frac{g_0}{g_1} \frac{\exp(\delta)/T}{[1 + (g_0/g_1) \exp(\delta/T)]^2}, \quad (4)$$

where δ is the energy difference in units of K between the two levels, and g_0 and g_1 are the degeneracies of the ground state and first excited state [24]. The crystal structure of PrFePO belongs to the $p4/nmm$ space group, with Pr^{3+} ions at the points of a tetragonal unit cell [1]. The energy level scheme for a Pr ion for the tetragonal symmetry CEF Hamiltonian contains 5 singlets and 2 doublets [25]. As shown in figure 3, the best fit to the data suggests that both the ground state and first excited states are nonmagnetic singlets. It is also clear that, for unannealed specimens, equation 3 overestimates the value of γ . In contrast, the $C(T)/T$ data for O_2 -annealed samples are fit extremely well for $2 \text{ K} < T < 45 \text{ K}$ and γ is only slightly overestimated. These results suggest that for the unannealed sample, there are a range of CEF energy level splittings which broaden the Schottky peak and render equation 3 too simple an expression to adequately describe

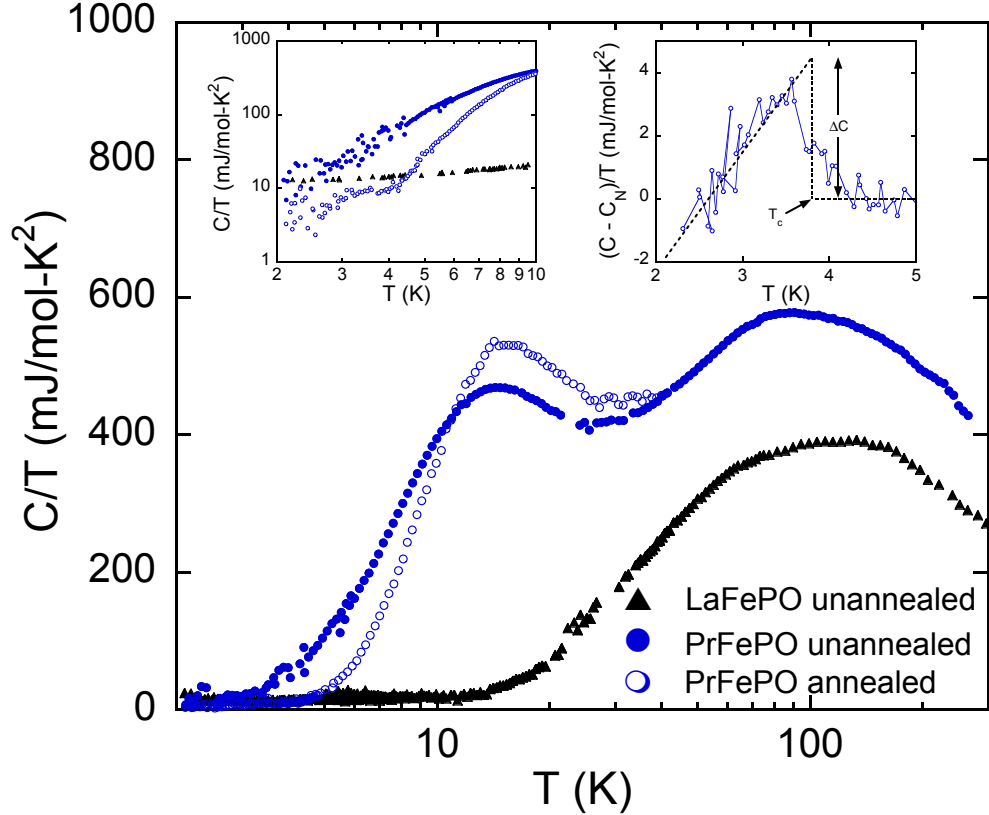


Figure 2. Linear-log plot of specific heat divided by temperature C/T versus temperature T for unannealed LaFePO , unannealed PrFePO and O_2 -annealed PrFePO . Left inset: Log-log C/T versus T plot for unannealed LaFePO , unannealed PrFePO and O_2 -annealed PrFePO at low T . For O_2 -annealed PrFePO , a broad jump is seen near $T_c = 3.6$ K. Right inset: C/T versus T plot where the normal state electronic contribution has been subtracted, revealing the jump associated with the superconducting transition. The dotted line represents an equal entropy construction that was used to determine the value of T_c and the size of the jump ΔC .

the data. It is possible that a range of CEF energy splittings could arise as the result of crystalline disorder which would introduce variation in the local charge distribution around individual Pr ions. Thus, it seems likely that O_2 -annealing reduces the spread of CEF energy level splittings, resulting in a sharper Schottky peak and a better CEF fit for O_2 -annealed samples. For the unannealed and O_2 -annealed PrFePO samples, the splitting between the ground state and the first excited state is 41.2 K and 48.4 K, respectively. The remaining fit parameters are summarized in table 2.

As shown in the left inset to figure 2, γ approaches 12.7 and 10 mJ/mol-K^2 for unannealed LaFePO and PrFePO , respectively, and 3 mJ/mol-K^2 for O_2 -annealed PrFePO , as T goes to zero. For both unannealed LaFePO and PrFePO , there is no detectable jump in the specific heat near the superconducting transition temperatures inferred from $\rho(T)$. In contrast, the O_2 -annealed PrFePO specimen shows a broad jump at low T . In order to determine T_c and the size of the specific heat jump ΔC

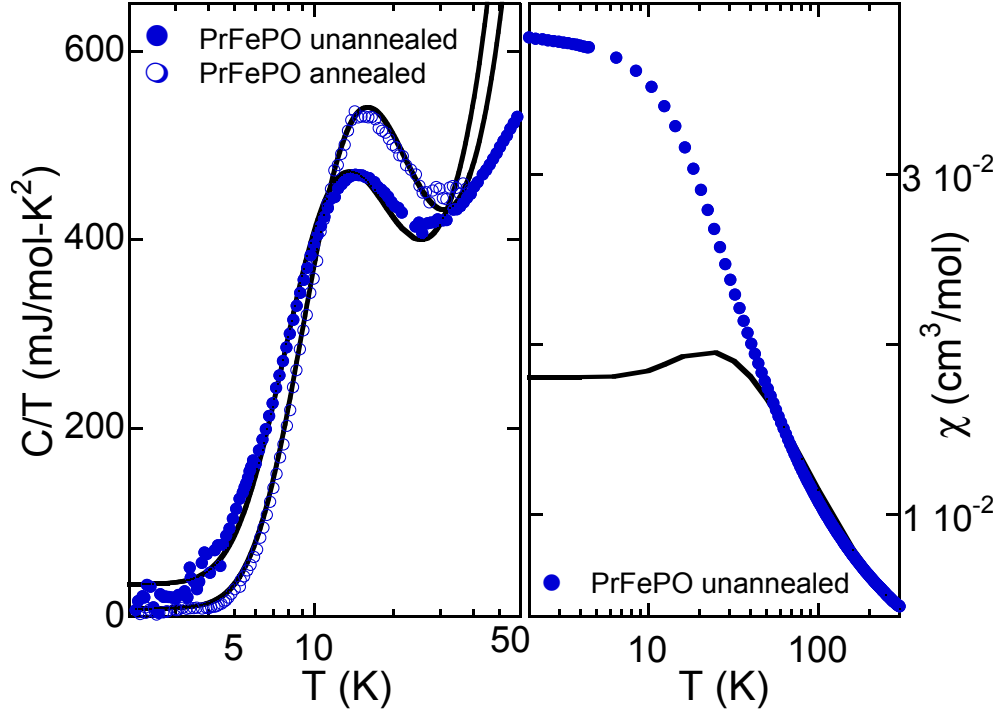


Figure 3. Left panel: Specific heat divided by temperature C/T versus T for unannealed and O_2 -annealed PrFePO. The solid lines are fits to the data using equation 3. Right panel: Magnetic susceptibility $\chi(T) = M/H$ data for unannealed PrFePO. The solid line is a fit to the data using equation 7.

for O_2 -annealed PrFePO, the normal state terms were subtracted from C/T near the discontinuity, resulting in the curve shown in the right inset to figure 2. The parameters, T_c and ΔC were then determined by applying an equal entropy construction, as shown by the dashed line in the right inset to figure 2. In agreement with $\rho(T)$ for unannealed samples, $T_c = 3.6$ K. Interestingly, the specific heat jump $\Delta C = 15.1$ mJ/mol-K is nearly 100 % of the value expected for a weak-coupling conventional BCS superconductor, given by $\Delta C = 1.52\gamma T_c = 16.4$ mJ/mol-K if γ is the extrapolated value of 3 mJ/mol-K^2 and $T_c = 3.6$ K [26]. In comparison, unannealed LaFePO and PrFePO are expected to show $\Delta C = 127.4$ and 54.7 mJ/mol-K , respectively. By comparing the expected specific heat jumps with the scatter in the $C(T)$ data for the unannealed samples, it appears that at most $\sim 40\%$ of the bulk is superconducting for the unannealed samples.

The normal state $\chi(T)$ data for unannealed LaFePO, PrFePO, and NdFePO are shown in figure 4. Near ~ 220 K, $\chi(T)$ increases strongly with decreasing T for LaFePO and NdFePO. This temperature dependence is similar to that of the compound Fe_2P [27], which may be present as inclusions or surface impurities. We estimate that our observed magnetic susceptibility is consistent with 1-2% Fe_2P impurity for both LaFePO and NdFePO. Interestingly, the $\chi(T)$ data for PrFePO show no such feature. With decreasing T , $\chi(T)$ for LaFePO increases gradually and exhibits a low T upturn which persists down to 2 K. This behavior is not typical for Fe_2P , and is either intrinsic to

Table 2. A summary of results from specific heat measurements for the compounds $LnFePO$ where $Ln = La, Pr$. For γ , both the extrapolated $T = 0K$ value and the results from CEF fits (equation 3) are reported. The additional parameters from fits to the data using equation 3 are the coefficient β of the phonon contribution, the splitting of the ground and first excited states by the crystalline electric field $\delta(K)$, and the fitting parameter r .

Ln	$\gamma(\text{mJ/mol-K}^2)$	$\gamma_{CEF}(\text{mJ/mol-K}^2)$	$\beta(\text{mJ/mol-K}^4)$	$\delta(K)$	r
La unannealed	12.7	—	0.10	—	—
Pr unannealed	10	33	0.28	41.2	1.57
Pr O ₂ -annealed	3	7.3	0.22	48.4	2.27

LaFePO or due to a small concentration of some other paramagnetic impurity. For unannealed NdFePO, $\chi(T)$ is consistent with Curie-Weiss behavior for Nd^{3+} ions for $2 K < T < 150 K$, where the magnetic contribution from the magnetic ordering at 220 K appears to be constant. For this T range, $\chi(T)$ can be described by a sum of a constant term and Curie-Weiss function and is given by the expression,

$$\chi(T) = \chi_0 + C/(T - \Theta) \quad (5)$$

where $\chi_0 = 0.039 \text{ cm}^3/\text{mol}$, $C = 1.33 \text{ cm}^3\text{K}/\text{mol}$, and $\Theta = -8.1 \text{ K}$. The χ_0 term is unusually large and it seems likely it may be attributed to the magnetic contribution of the impurity phase. From the Curie constant C , it appears that the effective magnetic moment for the Nd ions is $3.26 \mu_B$, which is reasonably close to the value expected for Nd^{3+} ions according to Hund's rules ($\mu_{eff} = 3.62 \mu_B$ for Nd^{3+}). Lastly, the negative Curie-Weiss temperature indicates antiferromagnetic spin correlations for the Nd ions.

Similarly, $\chi(T)$ for unannealed PrFePO shows behavior that is consistent with Curie-Weiss behavior for $50 K < T < 300 K$ and is described by equation 5, where $\chi_0 = 0$, $C = 1.58 \text{ cm}^3\text{K}/\text{mol}$, and $\Theta = -46.7 \text{ K}$. Again, the Curie constant yields a reasonable value of $\mu_{eff} = 3.55 \mu_B$ ($\mu_{eff} = 3.58 \mu_B$ for Pr^{3+} according to Hund's rules), while the large negative Curie-Weiss temperature indicates antiferromagnetic spin correlations for the Pr ions. For $T < 50 K$, $\chi(T)$ is suppressed from Curie-Weiss behavior and saturates to a constant value with decreasing T . This result is consistent with the ground and first excited states being nonmagnetic singlets, between which the energy splitting is close to 41 K as inferred from the fit to the Schottky anomaly in the $C(T)/T$ data. In order to describe the effect of crystalline electric field splitting on $\chi(T)$, a CEF fitting scheme is considered. As mentioned above, the crystal structure of PrFePO belongs to the $p4/nmm$ space group, with Pr^{3+} ions at the points of a tetragonal unit cell. The crystalline electric field (CEF) Hamiltonian of the Pr ions has the form

$$\mathcal{H}_{CEF} = B_2^0 O_2^0 + B_4^0 O_4^0 + 5B_4^0 O_4^4 + B_6^0 O_6^0 - 21B_6^0 O_6^4, \quad (6)$$

where O_2^0 , O_4^0 , O_4^4 , O_6^0 , and O_6^4 are Stevens operators for the $J = 4$ manifold and the B s are parameters determined from experiment. The CEF Hamiltonian \mathcal{H}_{CEF} splits the $J = 4$ Hund's rule multiplet of Pr^{3+} into 5 singlets and 2 doublets. In the presence of an

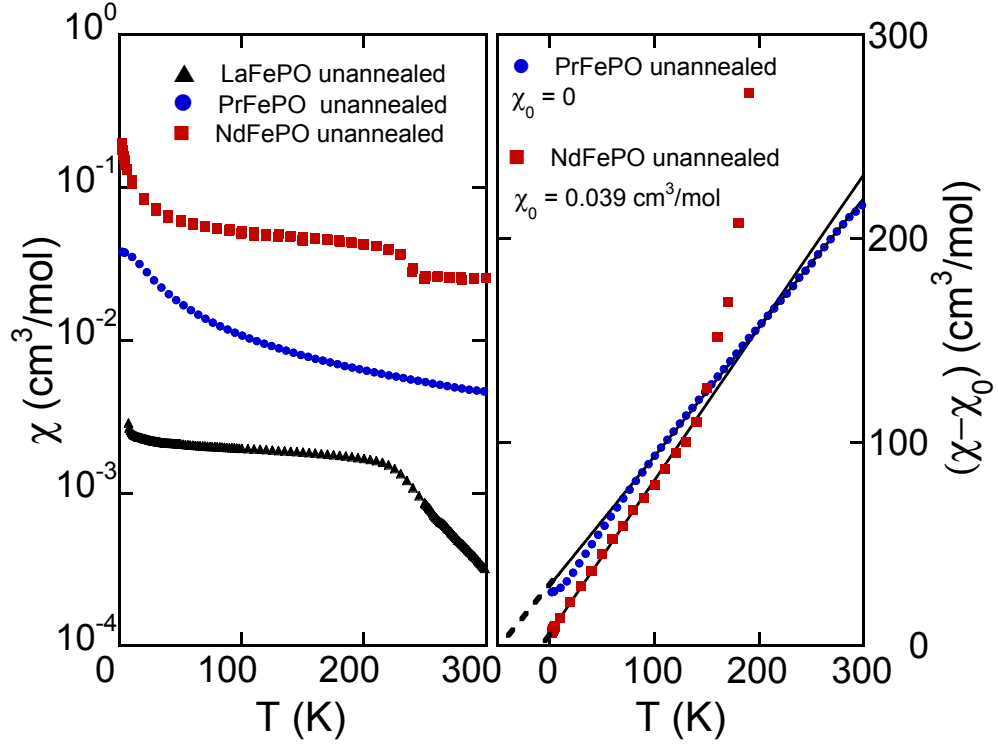


Figure 4. Left panel: Magnetic susceptibility $\chi(T) = M/H$ versus T for LnFePO ($\text{Ln} = \text{La}, \text{Pr}, \text{Nd}$) data. Right panel: Inverse magnetic susceptibility χ^{-1} versus T for LnFePO ($\text{Ln} = \text{Pr}, \text{Nd}$). The straight lines are fits to the data using modified Curie-Weiss expressions, as given by equation 5.

external magnetic field, the Zeeman interaction mixes and splits the CEF energy levels and the magnetic susceptibility is given by [28]

$$\chi_{\text{CEF}} = \frac{\sum_n \left[(E_n^{(1)})^2/kT - 2E_n^{(2)} \right] \exp(-E_n^{(0)}/kT)}{\sum_n \exp(-E_n^{(0)}/kT)}, \quad (7)$$

where the $E_n^{(0)}$ are the unperturbed cubic CEF levels, $E_n^{(1)} = \mu_B g \langle \phi_n | J | \phi_n \rangle$ with ϕ the CEF wave functions and g the Landé g -factor, and

$$E_n^{(2)} = \sum_{n' \neq n} \mu_B^2 g^2 \frac{|\langle \phi_n | J | \phi_{n'} \rangle|^2}{E_n^{(0)} - E_{n'}^{(0)}}. \quad (8)$$

In the molecular-field approximation, the measured magnetic susceptibility χ is given by $\chi = \chi_{\text{CEF}}/(1 - \lambda\chi_{\text{CEF}})$, where λ is the molecular field parameter that describes exchange interactions between Pr^{3+} ions [29]. Our best fit is shown as the solid curve in figure 3 where it is apparent that the CEF fit only describes the data qualitatively. The CEF fit parameters are $B_2^0 = -1.1$ meV, $B_4^0 = 0.0001$ meV, $B_4^4 = 0.0082$ meV, $B_6^0 = -0.0030$ meV, $B_6^4 = -0.0148$ meV, and $\lambda = -18.4$ mol/emu. This set of CEF parameters suggests the energy separation between the ground and first excited states is 44.3 K, and both

ground and first excited states are singlets, in good agreement with the specific heat data.

In an effort to determine whether the superconductivity is a bulk phenomenon, zero-field-cooled (ZFC) and field-cooled (FC) measurements of the magnetic susceptibility were made in a field of 5 Oe for unannealed and O_2 -annealed LaFePO, PrFePO, and NdFePO crystals. It should be noted at the outset that the values of $M(\text{emu/g})$ are accurate to roughly $\pm 15\%$ due to uncertainties in mass and geometry of the small crystals. A plot of the ZFC and FC magnetic susceptibility through the superconducting transition temperatures observed in $\rho(T)$ is shown in figure 5. For unannealed LaFePO, the onset temperature for LaFePO is near 6.0 K. With O_2 -annealing, T_c increases to a value near 7.0 K. For both the unannealed and O_2 -annealed cases, the FC data return to $\sim 5\%$ of the ZFC values. It also appears that the normal state magnetization is slightly enhanced for the O_2 -annealed samples. Unannealed PrFePO shows a weak superconducting transition near 2 K for ZFC measurements and the FC measurement reveals a weak upturn in the magnetization below T_c . Although this feature is anomalous for typical superconductors, it has been repeatedly observed for these crystals. With annealing, PrFePO develops a pronounced superconducting transition with an onset near $T_c = 4.4$ K which is again accompanied by the anomalous low T upturn in the FC measurement. Interestingly, the normal state magnetization is markedly enhanced for the O_2 -annealed samples. A comparison of our specific heat, magnetic susceptibility, and resistivity measurements on PrFePO is shown in figure 6. Unannealed NdFePO shows no evidence for a superconducting transition down to 2 K. Again, O_2 -annealing promotes superconductivity, yielding an onset temperature $T_c = 4.4$ K. For O_2 -annealed NdFePO, the FC data return to $\sim 3\%$ of the ZFC values. Also, there is no offset in the normal state magnetization as the result of O_2 -annealing. Thus, it is evident that O_2 -annealing acts to promote the superconducting state for LaFePO, PrFePO, and NdFePO, although it is unclear what the overall effect of O_2 -annealing is on the normal state behavior. Additionally, the small recovery of the diamagnetic signal on field-cooling indicates either that the material shows strong vortex pinning or that the superconductivity is not a bulk phenomenon. Further studies are required to make this distinction.

4. Discussion

An important question for understanding the Fe- Pn superconductors is how the magnetism associated with the Ln ion influences the superconductivity. For conventional superconductors, it is expected that T_c values are suppressed by the introduction of magnetic ions, as is observed for the well known case of de Gennes' scaling in BCS superconductors [30, 31]. Interestingly, both the series $LnFeAsO_{1-x}F_x$ and $LnFeAsO_{1-\delta}$ display an increase in the maximum T_c values on replacing La with magnetic Ln ions [3, 4, 5, 6, 8]. This result, together with the apparent suppression of a spin density wave that is correlated with the appearance of superconductivity,

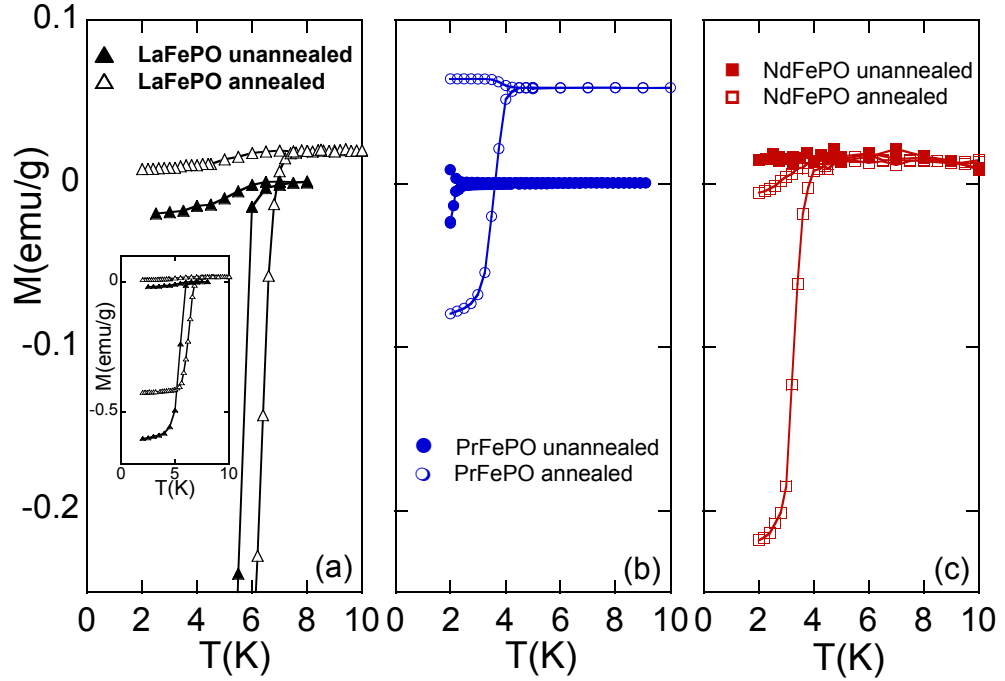


Figure 5. Left panel: Magnetization $M(T)$ data for $H = 5$ Oe for unannealed and O_2 -annealed LaFePO samples. Center panel: Magnetization $M(T)$ data for $H = 5$ Oe for unannealed and O_2 -annealed PrFePO samples. Right panel: Magnetization $M(T)$ data for $H = 5$ Oe for unannealed and O_2 -annealed NdFePO samples.

has led to the suggestion that the superconductivity exhibited by these compounds is unconventional in the sense that it is promoted by magnetic interactions [32]. In contrast, for the series $LnFePO$, the T_c values decrease upon replacing La with Pr, Nd, or Sm, as could be expected for a conventional superconductor in the presence of magnetic pairbreaking interactions. For the purpose of comparison, the evolution of T_c versus Ln for the series $LnFeAsO_{1-x}F_x$, $LnFeAsO_{1-\delta}$, and $LnFePO$ is shown in figure 7. While one should be careful when comparing systematics between undoped $LnFePO$ and optimally doped $LnFeAsO_{1-x}F_x$ and $LnFeAsO_{1-\delta}$ samples, the opposite effects of magnetic ion substitution could be taken as evidence for a difference between the P- and As-based compounds in the mechanism of superconductivity. The point of view that the superconductivity for the series $LnFePO$ is BCS-like is supported by the lack of anomalous behavior in the electrical resistivity, magnetic susceptibility, and specific heat.

Another important question for understanding the Fe- Pn superconductors is how sample quality affects the superconductivity. Broadly speaking, sample quality can be defined as either crystalline or chemical homogeneity, each of which has the potential to affect the physical properties in unique ways. It has been noted [33] that among several samples of undoped LaFePO, those with the lowest residual resistivities display the highest T_c values. A correlation between low residual resistivity and high T_c has also been observed in SmFePO [16]. This trend could derive from several possible differences

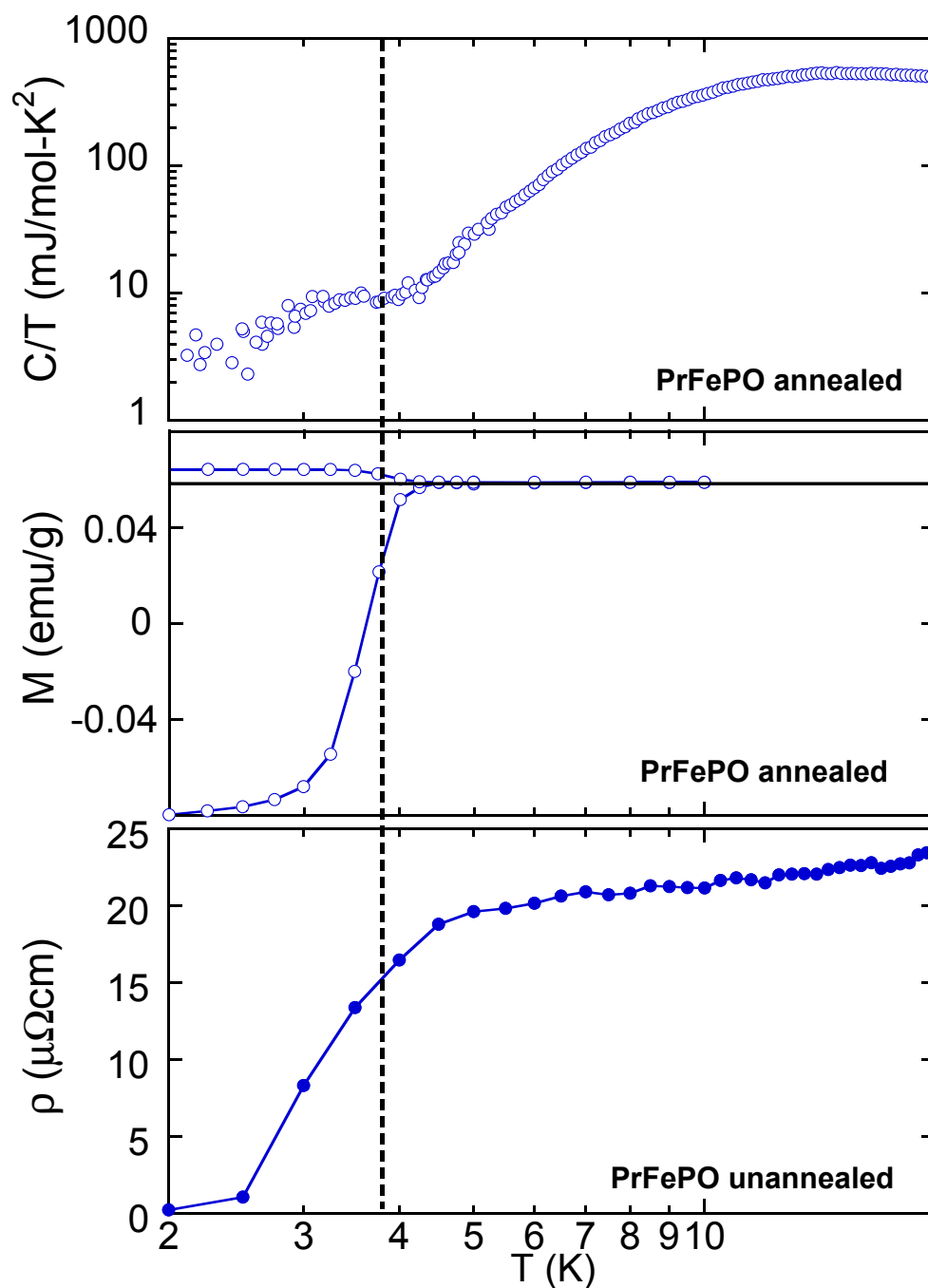


Figure 6. A comparison of the electrical resistivity ρ versus T data for unannealed PrFePO samples with specific heat divided temperature C/T versus T and magnetization M versus T for O_2 -annealed PrFePO showing the agreement in T_c among the measurements.

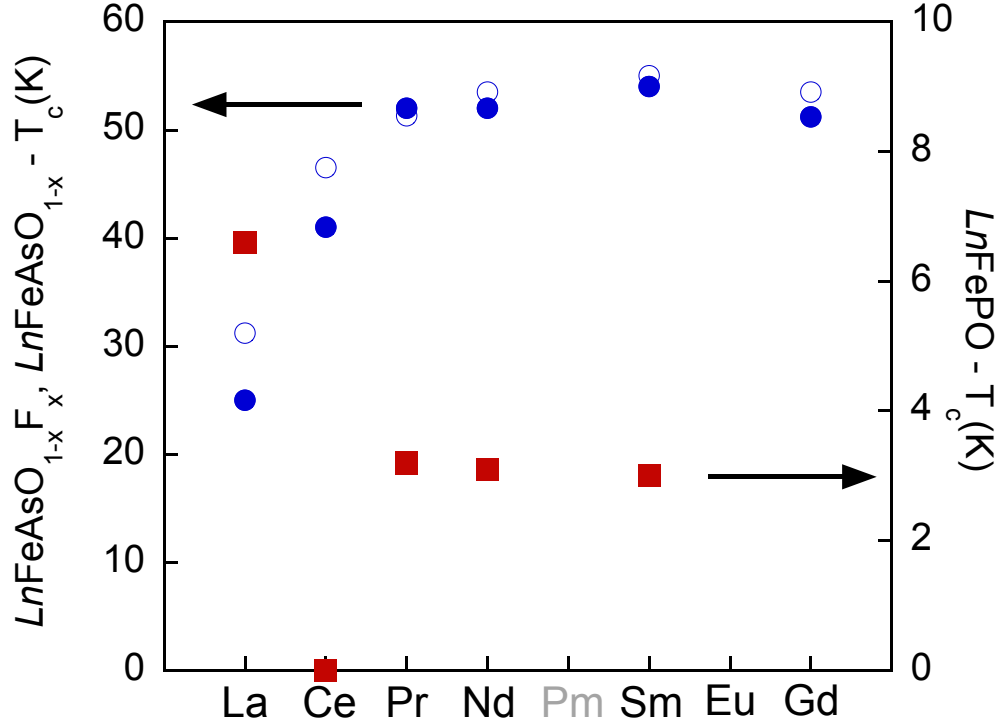


Figure 7. A comparison of the evolution of the superconducting transition temperature T_c versus lanthanide Ln for the series LnFePO with $\text{Ln} = \text{La}, \text{Ce}$ [17], $\text{Pr}, \text{Nd}, \text{Sm}$ [16] (solid squares), the optimally fluorine doped compounds $\text{LnFeAsO}_{1-x}\text{F}_x$ with $\text{Ln} = \text{La}$ [3], Ce [4], Pr [5], Nd [6], Sm [8], and Gd [9] (solid circles), and the oxygen deficient compounds $\text{LnFeAsO}_{1-\delta}$ [9] (open circles).

among the samples, including lattice disorder, oxygen vacancy induced changes in the carrier density, or oxygen vacancy induced changes in the lattice parameters. Our measurements for LaFePO , PrFePO , and NdFePO , which clearly show that O_2 -annealing promotes the superconducting state, suggest a correlation between sample quality and higher T_c values. This is shown in figure 6 for PrFePO where electrical resistivity for unannealed samples, magnetization data for O_2 -annealed samples, and specific heat data for O_2 -annealed samples are compared. Comparison of magnetization data for unannealed and O_2 -annealed samples also show that superconductivity is promoted by O_2 -annealing (figure 5). In general, annealing tends to improve crystalline quality by allowing disorder in the lattice to relax, in addition to reducing possible chemical inhomogeneity. On the other hand, annealing can also promote phase separation. For this reason, although it seems reasonable to correlate crystalline quality with an enhancement of the superconducting state, it is still necessary to carry out a more systematic study of the effect of annealing in these compounds. Furthermore, we note that it may be possible to improve the superconducting properties of the Fe-As compounds by synthesizing high quality single crystal specimens.

5. Concluding Remarks

We have reported results for single crystals of the compounds $LaFePO$, $PrFePO$ and $NdFePO$, which were prepared by means of a flux growth technique. Measurements of electrical resistivity, magnetic susceptibility and specific heat reveal metallic behavior for unannealed samples, which evolves into a superconducting state at low T in $Ln = La$ ($T_c = 6.6$ K), $Ln = Pr$ ($T_c = 3.2$ K), and $Ln = Nd$ ($T_c = 3.1$ K). The effect of annealing in flowing O_2 at 700 °C for 24 hours was also studied and found to enhance the superconducting properties. Although it seems likely that the positive effect of O_2 -annealing on the superconducting properties is due to improved crystallinity and chemical homogeneity, further research will be required to support this conclusion. Finally, the evolution of T_c with Ln ion for the P- and As-based $LnFePnO$ compounds appears to be in opposite directions: T_c increases as Ln is varied from La to Sm for $Pn = As$ and decreases as Ln is varied from La to Sm for $Pn = P$. This suggests that the mechanism of the superconductivity in these two series of compounds may be different; i.e., the superconductivity may be unconventional for the arsenides and conventional for the phosphides.

5.1. Acknowledgments

The crystal growth work was supported by the U. S. Department of Energy (DOE) under research Grant DE FG02-04ER46105 and acquisition of crystal growth equipment was sponsored by the U. S. DOE through Grant DE FG02-04ER46178. Low temperature measurements were funded by the National Science Foundation (NSF) under Grant 0802478. The work of N. Crisosto was supported by the NSF through the Research Experience for Undergraduates (REU) program under grant PHY-0552402. The authors thank C. A. McElroy for experimental assistance with the specific heat measurements.

References

- [1] B. I. Zimmer, W. Jeitschko, J. H. Albering, R. Glaum, and M. Reehuis. The rare earth transition metal phosphide oxides $LnFePO$, $LnRuPO$ and $LnCoPO$ with $ZrCuSiAs$ type structure. *Journal of Alloys and Compounds*, 229:238, 1995.
- [2] Y. Kamihara, H. Hiramatsu, M. Hirano, R. Kawamura, H. Yanagi, T. Kamiya, and H. Hosono. Iron-based layered superconductor: $LaOFeP$. *Journal of the American Chemical Society*, 128:10012, 2006.
- [3] Y. Kamihara, T. Watanabe, M. Hirano, and H. Hosono. Iron-based layered superconductor $La[O_{1-x}F_x]FeAs$ ($x = 0.05 - 0.12$) with $T_c = 26$ K. *Journal of the American Chemical Society*, 130:3296, 2008.
- [4] G. F. Chen, Z. Li, D. Wu, G. Li, Z. Hu, J. Dong, P. Zheng, J. L. Luo, and N. L. Wang. Superconductivity at 41 K and its competition with spin-density-wave instability in layered $CeO_{1-x}F_xFeAs$. *Physical Review Letters*, 100:247002, 2008.
- [5] Z. A. Ren, J. Yang, W. Lu, W. Yi, G. C. Che, X. L. Dong, L. L. Sun, and Z.-X. Zhao. Superconductivity at 52 K in iron based F doped layered quaternary compound $Pr[O_{1-x}F_x]FeAs$. *Materials Research Innovations*, 12:105, 2008.

- [6] Z.-A. Ren, J. Yang, W. Lu, W. Yi, X. L. Shen, Z. C. Li, G. C. Che, X. L. Dong, L. L. Sun, F. Zhou, and Z. X. Zhao. Superconductivity in the iron-based F-doped layered quaternary compound $Nd[O_{1-x}F_x]FeAs$. *Europhysics Letters*, 82:57002, 2008.
- [7] X. H. Chen, T. Wu, R. H. Liu, H. Chen, and D. F. Fang. Superconductivity at 43 K in $SmFeAsO_{1-x}F_x$. *Nature*, 453:761, 2008.
- [8] Z. A. Ren, W. Lu, J. Yang, W. Yi, X. L. Shen, Z. C. Li, G. C. Che, X. L. Dong, L. L. Sun, F. Zhou, and Z. X. Zhao. Superconductivity at 55 K in iron-based F-doped layered quaternary compound $Sm[O_{1-x}F_x]FeAs$. *Chinese Physics Letters*, 25:2215, 2008.
- [9] J. Yang, Z.-C. Li, W. Lu, W. Yi, X.-L. Shen, Z.-A. Ren, G.-C. Che, X.-L. Dong, L.-L. Sun, F. Zhou, and Z.-X. Zhao. Superconductivity at 53.5 K in $GdFeAsO_{1-\delta}$. *Superconductor Science and Technology*, 21:082001, 2008.
- [10] A. S. Sefat, A. Huq, M. A. McGuire, R. Jin, B. C. Sales, D. Mandrus, L. M. D. Cranswick, P. W. Stephens, and K. H. Stone. Superconductivity in $LaFe_{1-x}Co_xAsO$. *Physical Review B*, 78:104505, 2008.
- [11] H.-H. Wen, G. Mu, L. Fang, H. Yang, and Y. Zhu. Superconductivity at 25 K in hole-doped $(La_{1-x}Sr_x)OFeAs$. *Europhysics Letters*, 82:17009, 2008.
- [12] C. Wang, L. Li, S. Chi, Z. Zhu, Z. Ren, Y. Li, Y. Wang, X. Lin, Y. Luo, S. Jiang, X. Xu, G. Cao, and Z. Xu. Thorium-doping-induced superconductivity up to 56 K in $Gd_{1-x}Th_xFeAsO$. *Europhysics Letters*, 83:67006, 2008.
- [13] Z.-A. Ren, G.-C. Che, X.-L. Dong, J. Yang, W. Lu, W. Yi, X.-L. Shen, Z.-C. Li, L.-L. Sun, F. Zhou, and Z.-X. Zhao. Superconductivity and phase diagram in iron-based arsenic-oxides $ReFeAsO_{1-\delta}$ ($Re = \text{rare-earth metal}$) without fluorine doping. *Europhysics Letters*, 83:17002, 2008.
- [14] M. Rotter, M. Tegel, and D. Johrendt. Superconductivity at 38 K in the iron arsenide $(Ba_{1-x}K_x)Fe_2As_2$. *Physical Review Letters*, 101:107006, 2008.
- [15] J. H. Tapp, Z. Tang, B. Lv, K. Sasmal, B. Lorenz, P. C. W. Chu, and A. M. Guloy. $LiFeAs$: An intrinsic $FeAs$ -based superconductor with $T_c = 18K$. *Physical Review B*, 78:060505(R), 2008.
- [16] Y. Kamihara, H. Hiramatsu, M. Hirano, Y. Kobayashi, S. Kitao, S. Higashitaniguchi, Y. Yoda, M. Seto, and H. Hosono. Coexistence of superconductivity and antiferromagnetic ordering in the layered superconductor $SmFePO$. *Physical Review B*, 78:184512, 2008.
- [17] E. M. Bruning, C. Krellner, M. Baenitz, A. Jesche, F. Steglich, and C. Geibel. $CeFePO$: A heavy fermion metal with ferromagnetic correlations. *Physical Review Letters*, 101:117206, 2008.
- [18] H. Okada, K. Igawa, H. Takahashi, Y. Kamihara, M. Hirano, H. Hosono, K. Matsubayashi, and Y. Uwatoko. Superconductivity under high pressure in $LaFeAsO$. *Journal of the Physical Society of Japan*, 77:113712, 2008.
- [19] M. Tegel, I. Schellenberg, R. Pöttgen, and D. Johrendt. A ^{57}Fe Moessbauer Spectroscopy Study of the 7 K Superconductor $LaFePO$. *arXiv:0805.1208*, 2008.
- [20] J. J. Hamlin, R. E. Baumbach, D. A. Zocco, T. A. Sayles, and M. B. Maple. Superconductivity in single crystals of $LaFePO$. *Journal of Physics: Condensed Matter*, 20:365220, 2008.
- [21] T. M. McQueen, M. Regulacio, A. J. Williams, Q. Huang, J. W. Lynn, Y. S. Hor, D. V. West, M. A. Green, and R. J. Cava. Intrinsic properties of stoichiometric $LaOFeP$. *Physical Review B*, 78:024521, 2008.
- [22] J. G. Analytis, J. H. Chu, A. S. Erickson, C. Kucharczyk, A. Serafin, A. Carrington, C. Cox, S. M. Kauzlarich, H. Hope, and I. R. Fisher. Bulk superconductivity and disorder in single crystals of $LaFePO$. *arXiv:0810.5368*, 2008.
- [23] C. Krellner and C. Geibel. Single crystal growth and anisotropy of $CeRuPO$. *Journal of Crystal Growth*, 310:1875, 2008.
- [24] E. S. R. Gopal. *Specific Heat at Low Temperatures*. Plenum Press, New York, 1966.
- [25] R. Michalski, Z. Ropka, and R. J. Radwanski. Crystal-field interactions in $PrRu_2Si_2$. *Journal of Physics: Condensed Matter*, 12:7609, 2000.
- [26] J. Bardeen, L. N. Cooper, and J. R. Schrieffer. Theory of superconductivity. *Physical Review*,

- 108:1175, 1957.
- [27] D. Bellavance, J. Mikkelsen, and A. Wold. Preparation and properties of Fe_2P . *Journal of Solid State Chemistry*, 2:285, 1970.
- [28] J. H. van Vleck. *Electric and Magnetic Susceptibility*. Oxford, New York, 1932.
- [29] T. Murao and T. Matsubara. On the magnetic properties of cubic cerium. *Progress in Theoretical Physics*, 18:215, 1957.
- [30] P. G. De Gennes. Interactions indirectes entre couches 4f dans les metaux de terres rares. *Journal de Physique et Le Radium*, 23:510, 1962.
- [31] M. B. Maple, L. E. DeLong, and B. C. Sales. *Handbook on the Physics and Chemistry of Rare Earths*, chapter 11, page 797. North-Holland Publishing Company, 1978.
- [32] A. J. Drew, F. L. Pratt, T. Lancaster, S. J. Blundell, P. J. Baker, R. H. Liu, G. Wu, X. H. Chen, I. Watanabe, V. K. Malik, A. Dubroka, K. W. Kim, M. Rössle, and C. Bernhard. Coexistence of magnetic fluctuations and superconductivity in the pnictide high temperature superconductor $\text{SmFeAsO}_{1-x}\text{F}_x$ measured by muon spin rotation. *Physical Review Letters*, 101:097010, 2008.
- [33] Y. Kamihara, M. Hirano, H. Yanagi, T. Kamiya, Y. Saitoh, E. Ikenaga, K. Kobayashi, and H. Hosono. Electromagnetic properties and electronic structure of the iron-based layered superconductor LaFePO . *Physical Review B*, 77:214515, 2008.